B. Jacod
email: b.c.jacod@wb.utwente.nl

C. H. Venner

University of Twente,
Faculty of Mechanical Engineering,
P.O. Box 217, NL 7500 AE Enschede,
The Netherlands

P. M. Lugt
SKF Engineering and Research Center B. V.,
P.O. Box 2350, NL 3430 DT Nieuwegein,
The Netherlands

A Generalized Traction Curve for EHL Contacts

In this paper the subject of friction prediction is revisited, with the aim of obtaining a general formula predicting the coefficient of friction over a wide range of operating conditions. By means of full numerical simulations of the smooth isothermal elliptic contact, and assuming an Eyring non-Newtonian behavior, the coefficient of friction is computed for a wide range of operating conditions. It is shown that with respect to sliding friction, all results can be presented on a single generalized friction curve relating a reduced coefficient of friction to a characteristic nondimensional shear stress. Finally, it is shown that some measured data presented in the literature when presented in terms of the derived parameters closely follow the derived behavior, which provides a validation of the theoretical results. [DOI: 10.1115/1.1308021]

I Introduction

The thickness of the lubricant film separating two surfaces of an elastohydrodynamically lubricated (EHL) contact is of crucial importance for the successful operation of the contact. The accurate prediction of the film thickness as a function of the operating conditions has therefore received much attention in the literature. For ideally smooth surfaces, the film thickness can already be predicted quite accurately with the widely used formulas of Dowson and Higginson [1] and Hamrock and Dowson [2]. Recent improvements of both numerical and experimental tools allow an increasingly deep insight into the effects of surface roughness (see Lubrecht and Venner [3] and references therein for the numerical part, and Spikes [4] and Kaneta and Nishikawa [5] for reviews of experimental progress).

Compared to the amount of work dedicated to film thickness formula in EHL contacts, very little attention has been paid to the development of formulas to predict the coefficient of friction. However, for industrial applications accurate prediction of the friction is of equal importance, as it determines the power loss in the contact and the efficiency of machine components, e.g., bearings. Moreover, an accurate prediction of the coefficient of friction is of the utmost importance for the further development of applications such as variable transmission which specifically rely on the control of the shear in the lubricant.

The reasons for such a late development are twofold. By contrast with the film thickness, which is essentially determined at the inlet, friction originates in the center of the contact where the conditions are such that the rheological behavior of the lubricant film has long been unclear. The debate is not closed yet, but the main characteristics of lubricant behavior are now taken into account in generally accepted models; see Johnson and Tevaarwerk [6], Bair and Winer [7], and Evans and Johnson [8]. Concurrently, the incorporation of non-Newtonian rheology in the EHL contact model has proved to be difficult for general elliptical contacts. As a result, most solvers for the EHL problem, incorporating non-Newtonian lubricant behavior have been restricted to the line contact, and most point contact predictions are based on approximate formulas derived from simplified film thickness and pressure solutions.

Examples of non-Newtonian EHL line contact studies are given by Jacobson and Hamrock [9], Houpert and Hamrock [10], Conry, Wang, and Cusano, [11], Lee and Hamrock [12], Sui and Sadeghi [13], and Hsiao and Hamrock [14]. In those studies, however, computed values of friction are presented only for a few isolated cases, and no attempt is made to derive a general formula to predict traction as a function of the operating conditions. The same applies to the few studies dealing with the full numerical simulation of non-Newtonian elliptical contacts, where little attention was paid to the prediction of traction as a function of the governing parameters in a systematic way; see Kim and Sadeghi [15] and Holt, Evans, and Snidle [16]. As a result, with respect to the prediction of traction one has to rely on results obtained using approximate approaches where specific assumptions are made regarding the pressure profile and film shape; see Evans and Johnson [17] and Olver and Spikes [18]. However, it should be noted that these latter studies at least have shed some light on the characteristic parameters that determine friction in the contact.

In this paper both a complete solution of the non-Newtonian elliptical contact and the development of simple formulas for predicting friction are addressed. It is shown by full numerical simulations for varying load conditions, lubricant parameters, and contact geometry (including line contacts) that all computed friction results can be represented on a single ''mastercurve,'' giving a reduced friction coefficient as a function of a nondimensional shear stress. This strongly suggests that a unifying mechanism exists that governs the friction in EHL contacts. This claim is supported by the fact that experimental friction coefficients available in the literature, when plotted as a function of the identified parameters, closely follow the obtained mastercurve.

II Problem Presentation

A Equations. The equations have been nondimensionalized using the Hertzian dry contact parameters and the lubricant properties at ambient pressure; see Nomenclature. Effective viscosities are introduced to account for the effects of non-Newtonian lubricant behavior. The dimensionless Reynolds equation for the elliptic contact can be written as

$$\frac{\partial}{\partial X}\left(\frac{\overline{\rho}H^3}{\lambda\,\overline{\eta}_X}\frac{\partial P}{\partial X}\right)+\kappa^2\frac{\partial}{\partial Y}\left(\frac{\overline{\rho}H^3}{\lambda\,\overline{\eta}_Y}\frac{\partial P}{\partial Y}\right)-\frac{\partial(\overline{\rho}H)}{\partial X}=0, \qquad (1)$$

with the boundary conditions $P=0$, and the cavitation condition $P\geqslant 0$ everywhere. In this equation κ is the aspect ratio of the Hertzian contact ellipsoid,

$$\kappa=a/b,$$

and λ a dimensionless speed parameter:

$$\lambda=(6\,\eta_0 u_s a)/(c^2 p_H).$$

$\overline{\eta}_X$ and $\overline{\eta}_Y$ are the effective viscosities in the X and Y direction, respectively. For the line contact problem and various types of

Contributed by the Tribology Division of THE AMERICAN SOCIETY OF MECHANICAL ENGINEERS for presentation at the STLE/ASME Tribology Conference, Seattle, WA, October 1–4. Manuscript received by the Tribology Division Jan. 25, 2000; revised manuscript received June 8, 2000. Paper No. 2000-TR1B-11. Associate Editor: B. O. Jacobson.

non-Newtonian behavior, an expression for the effective viscosity can be derived analytically; see Refs. [11], [12], and [19]. However, for the point contact problem, this is not possible. A way around this is to use approximate expressions derived from a perturbation approach; see Ref. [20]. For the case of the Eyring model this leads to the following expressions for dimensionless effective viscosities:

$$\bar{\eta}_X = \bar{\eta}/\cosh(\bar{\tau}_m), \tag{2}$$

$$\bar{\eta}_Y = \bar{\eta}/(\bar{\tau}_m \sinh(\bar{\tau}_m)), \tag{3}$$

where the dimensionless mean shear stress is given by

$$\bar{\tau}_m = \sinh^{-1}\left(\mathcal{N}\frac{\bar{\eta}\bar{S}}{H}\right), \tag{4}$$

with

$$\mathcal{N} = \frac{\lambda p_H^2 \mathcal{K}}{6E'\tau_0}.$$

The perturbation analysis is based on the assumption that the shear stresses are only partially coupled, $\tau_e = \tau_x = \tau_m + z(\partial p/\partial x)$ and that the mean shear stress in the y direction is negligible, so $\tau_y = z(\partial p/\partial y)$, where z varies from $(-h/2)$ to $(+h/2)$. For details regarding to the perturbation analysis the reader is referred to Refs. [20] and [21].

In its simplest form the lubricant density is assumed to be constant $\bar{\rho}=1$, and the viscosity is taken to depend on the pressure according to the Barus equation. In dimensionless form, this equation is given by

$$\bar{\eta} = \exp(\bar{\alpha}P), \tag{5}$$

Alternatively the variations of the density with pressure can be modeled with the Dowson and Higginson relation [1], and the Roelands viscosity pressure equation [22] can be used.

The dimensionless film thickness equation is given by

$$H(X,Y) = \Delta + \mathcal{S}X^2 + (1-\mathcal{S})Y^2 + \frac{1}{\pi\mathcal{K}}\int\int_S \frac{P(X',Y')dX'dY'}{\sqrt{\kappa^2(X-X')+(Y-Y')}}, \tag{6}$$

where $\mathcal{S}=\mathcal{S}(\kappa)$ is a shape factor due to the ellipticity of the contact (see Sec. I), and Δ is an integration constant determined by the force balance condition:

$$\int\int_S PdXdY = \frac{2\pi}{3} \tag{7}$$

Finally, the reduced coefficient of friction is defined as

$$\bar{\mu} = \mu\frac{p_H}{\tau_0} = \frac{\int\int_S \bar{\tau}_x dXdY}{\int\int_S PdXdY}. \tag{8}$$

B Control Parameters. The aim of this paper is to map the coefficient of friction as a function of the operating conditions, and to obtain a simple and accurate description for use in practice. For the simplest case of an incompressible lubricant obeying the Barus equation, it can be easily inferred from the equations given in Sec. III A that $\bar{\mu}$ is a function of $\bar{\alpha}$, λ, κ, and $\mathcal{N}$. Alternatively, the so-called Moes parameters derived using optimum similarity analysis could be used; see Moes [23]. In that case one obtains four parameters, M, L, D (please refer to Nomenclature), and

$$\bar{S} = S\left(\frac{u_s\eta_0 E'}{\tau_0^2 R_x}\right)^{1/2}. \tag{9}$$

For the circular contact $(D=1)$, it follows that $\bar{\mu}$ is a function of M, L, and $\bar{S}$ only. The specific form of the relation $\bar{\mu} = f(M,L,\bar{S})$ is first investigated for this simplest case. Subsequently the changes brought about by the introduction of compressibility and the replacement of Barus viscosity pressure relation by the more realistic Roelands relation are studied. Finally, the effects of contact ellipticity are considered.

III Friction Calculations

The investigation is conducted using a multigrid solver incorporating non-Newtonian effects. The numerical details and an indication of the numerical accuracy of the analysis are presented in the Appendix.

A Barus-incompressible Lubricant. A circular contact using an incompressible lubricant following Barus' viscosity pressure relation is first considered. For this problem the reduced coefficient of friction $\bar{\mu}$ has been computed for a wide range of conditions: $50 \leqslant M \leqslant 1000$, $1 \leqslant L \leqslant 15$, and $0.01 \leqslant S \leqslant 1$. A regression analysis is then performed on the computed friction data to derive a parameter, cluster of M, L, and $\bar{S}$, representing the severity of the operating conditions. The result of the analysis, $\bar{S}^{1/4}ML^3$, enables the computed friction coefficients to fall relatively closely on one curve for $\bar{S}^{1/4}ML^3 \geqslant 10^4$ while being scattered rather widely for lower values; see Fig. 1. A further examination shows, however, that $\bar{S}^{1/4}ML^3$ approximates the shear stress in the center of the contact. Expressing the central film thickness H_c and the dimensionless viscosity parameter $\bar{\alpha}$ as functions of M and L, (see Ref. [24]),

$$H_c = 1.7M^{-1/9}L^{3/4}, \tag{10}$$

one finds

$$\bar{S}^{1/4}ML^3 \sim c_1\left(\frac{\bar{S}\bar{\alpha}^{12}}{H_c}\right)^{1/4}. \tag{11}$$

Taking the high power of $\bar{\alpha}$ as an indication that the viscosity in the contact must be taken into account, it appears that the severity of the operating conditions should be represented by a characteristic shear stress:

$$\bar{\tau}_c = \frac{\bar{\eta}(p_H)\bar{S}}{H_c}. \tag{12}$$

Thus it seems that instead of expressing $\bar{\mu}$ as a function of M, L, and $\bar{S}$, it should be related to $\bar{\tau}_c$. This is confirmed by Fig. 2, where the calculational results are given in the form $\bar{\mu} = \bar{\mu}(\bar{\tau}_c)$. The results fall closely on a single curve which is approximately given by

$$\bar{\mu} = \sinh^{-1}(\bar{\tau}_c/5). \tag{13}$$

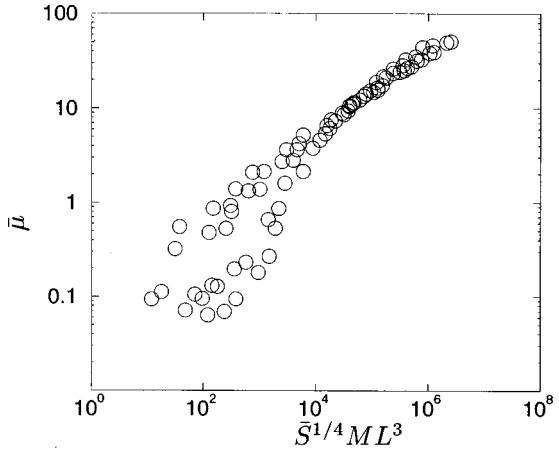

Fig. 1 Computed reduced friction coefficient, $\bar{\mu}$, as a function of the dimensionless parameter $\bar{S}^{1/4}ML^3$ for a Barus-incompressible lubricant.

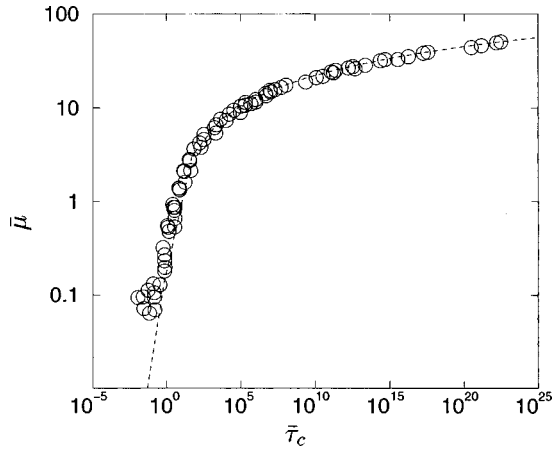

Fig. 2 Computed reduced friction coefficient $\bar{\mu}$ as a function of $\bar{\tau}_c$ for a Barus-incompressible lubricant. Dashed curve: Eq. (13).

However, for low values of $\bar{\tau}_c$, the results form a cluster of points straying away from the curve. This indicates that not all sources of friction are equally well represented by the parameters. This scattering at low values of $\bar{\tau}_c$ is explained by the fact that under these conditions (low slip) the rolling friction is dominant. Thus a parameter such as $\bar{\tau}_c$, based on the shear of the lubricant film in the center of the contact, cannot accurately characterize the frictional behavior. The use of $\bar{\tau}_c$ is therefore restricted to the sliding friction. This is confirmed by Fig. 3, where for the same cases as shown in Figs. 1 and 2 the computed reduced coefficient of friction based on the terms associated with sliding friction only is presented as a function of $\bar{\tau}_c$. That is, Fig. 3 was obtained by subtracting the contribution of the rolling friction. Consequently, in the rest of this work, coefficients of friction due only to sliding friction will be considered. For most practical applications the operating conditions are such that sliding friction prevails, and the rolling friction contribution can be neglected without significantly reducing the accuracy of the analysis.

Concluding this preliminary analysis, a set of parameters, $(\bar{\tau}_c, \bar{\mu})$ has been derived characterizing uniquely the coefficient of friction for the case of a circular contact and incompressible lubricant obeying the Barus viscosity pressure relation. The form of the parameters strongly suggests, however, that they may be equally well suited for all cases where the shear of the lubricant film in the center of the contact is the predominant source of friction. This means that results obtained when more realistic viscosity pressure equations are used or when the contact is no longer circular should follow the same behavior. This is investigated in the following sections.

Table 1 Lubricant properties. The viscosity at ambient pressure η_0, is given in mPa, and the pressure viscosity coefficient α in GPa^{-1}.

	Traction fluid		Mineral oil A		5P4E	
Temp (C^o)	α	η_0	α	η_0	α	η_0
40	28.7	28.4	21.6	8.24	35.0	266
60	22.8	13.1	18.6	4.19	26.3	79
100	16.5	4.6	15.4	2.01	14.9	15

Table 2 Range of variations of the parameters

p_H (GPa)	1	2	3
Temp. (^{o}C)	40	60	100
u_m (m/s)	2	7	12
S (%)	0.1	0.5	2
τ_0 (MPa)	4	6	8

B Varying Lubricant Properties. Coefficients of friction are first computed for varying lubricant properties while keeping the contact configuration circular. The lubricant parameters are taken to represent three widely different lubricants (see Table I): a mineral oil A, a traction fluid, and a polyphenyl ether (5P4E).

The conditions are now taken to be as close as possible to real traction tests conditions meaning that the lubricants are compressible and Roelands pressure-viscosity relation is preferred to Barus'. Operating conditions are varied widely with a maximum Hertzian pressure ranging from 1 to 3 GPa at temperatures of up to 100°C. Note that the temperature only affects the viscosity at ambient pressure. In all cases an isothermal contact is assumed. Therefore the variations of slip are kept in a small range to ensure that this assumption is justified (see Table II). These conditions can be translated in terms of M, L, and $\bar{S}$ using $R_x = 1.038\,75 \times 10^{-2}$ m and $E' = 226$ GPa. Finally, τ_0 is varied from 4 to 8 MPa to study its influence on friction, rather than taken at its real value as determined by experiments. The resulting reduced coefficients of friction are plotted as a function of $\bar{\tau}_c$ in Figs. 4, 5, and 6 (note that a log-linear scale is now used). For all three lubricants the

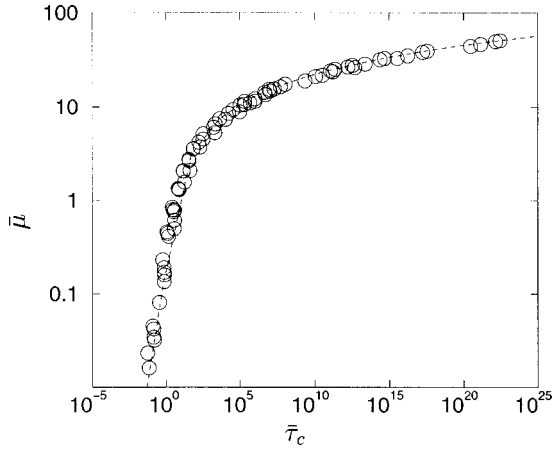

Fig. 3 Computed reduced sliding coefficient of friction $\bar{\mu}$ as a function of $\bar{\tau}_c$ for a Barus-incompressible lubricant. Dashed curve: Eq. (13).

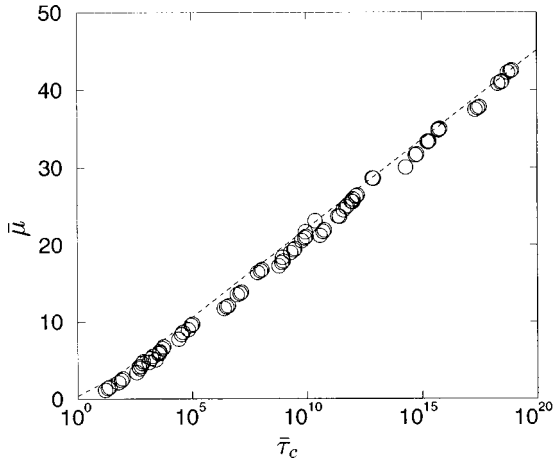

Fig. 4 Computed reduced sliding coefficient of friction $\bar{\mu}$ as a function of $\bar{\tau}_c$ for mineral oil *A*. Dashed curve: Eq. (13).

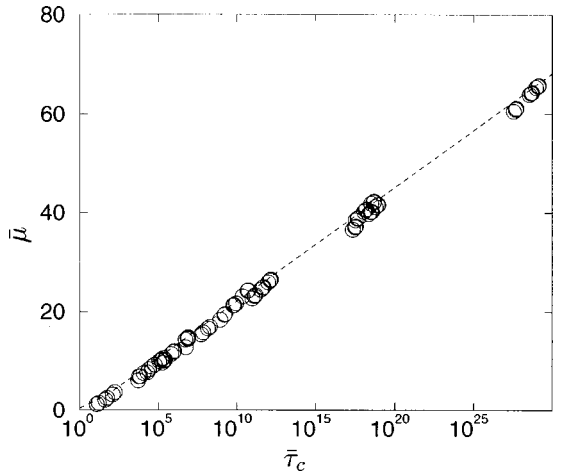

Fig. 5 Computed reduced sliding coefficient of friction $\bar{\mu}$ as a function of $\bar{\tau}_c$ for the traction fluid. Dashed curve: Eq. (13).

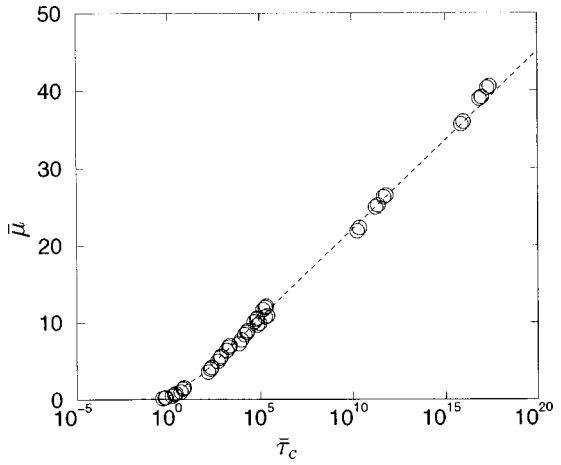

Fig. 6 Computed reduced sliding coefficient of friction $\bar{\mu}$ as a function of $\bar{\tau}_c$ for 5P4E. Dashed curve: Eq. (13).

Table 3 Cases considered in the investigation of the contact configuration influence

p_H (GPa)	Temp (^{o}C)	u_m (m/s)	S (%)	τ_0 (MPa)
1	60	12	2	8
2	100	2	0.1	6
2	40	7	0.1	8
3	60	12	0.1	4
3	40	7	0.1	8

friction data collapses on the mastercurve [Eq. (13)], thereby indicating that $\bar{\tau}_c$ and $\bar{\mu}$ are a very useful set of parameters to describe the frictional behavior, even for more general cases.

C Varying Contact Ellipticity. The mineral oil A is singled out and the influence of contact geometry investigated. The friction coefficients were computed for an elliptical contact with $R_x/R_y = 1/2$ and 1/5, and five load cases are chosen such as to cover the range of variation of the characteristic shear stress, $\bar{\tau}_c$, see Table III. In addition, using a separate approach based on the equations presented in Ref. [11] the same computations have been performed for a line contact configuration. The results of the

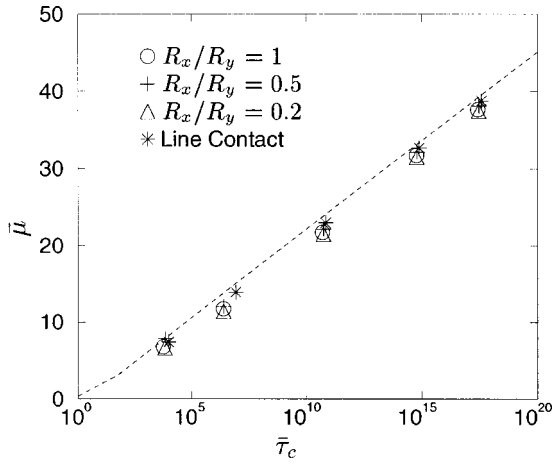

Fig. 7 Sliding friction results for different ellipticity ratios, mineral oil *A*. Dashed curve: Eq. (13).

elliptical and line contacts are presented in Fig. 7. All the data points closely follow the behavior predicted by Eq. (14). This implies that the two parameters $\bar{\mu}$ and $\bar{\tau}_c$ characterize the frictional behavior for a general contact geometry.

IV Experimental Validation

The close fit of Eq. (13) with the computed values of the reduced friction coefficient over a wide range of conditions encompassing several lubricants and ellipticity ratios indicates that $(\bar{\tau}_c, \bar{\mu})$ reflect a unified mechanism determining friction in EHL contacts. In this section, an experimental corroboration is sought by looking at experimental traction results presented in the literature, using $(\bar{\tau}_c, \bar{\mu})$ as a frame of analysis.

The present work is restricted to the Eyring model; thus the experimental results must come from tests where the lubricant follows an Eyring behavior and where the Eyring stress, τ_0, is measured. This limits the validation to data obtained from traction tests on two-disk machines.

Two sources are used here, Evans and Johnson [8,17] and Klein-Meuleman, Lubrecht, and ten Napel [25]. From the former, experimental coefficients of friction are extracted for a mineral oil B, the traction fluid used previously, and 5P4E under line contact conditions. The friction coefficients given in Figs. 2, 4, and 6 of Ref. [17] are transformed into $\bar{\mu}$ using τ_0 as given in Figs. 6, 7, and 8 of Ref. [8] under the conditions considered. Similarly, $\bar{\tau}_c$ is obtained from $\dot{\gamma}$ of Figs. 2, 4 and 6 of Ref. [17]: the value of the slip is extracted from $\dot{\gamma}$ using Dowson and Higginson's formula [1] for the film thickness, and the viscosity at the maximum Hertzian pressure is read on the experimental viscosity pressure graphs 3, 4, and 5 of Ref. [8]. In the experiments of Ref. [25], a circular contact using a third mineral oil (C) as lubricant is considered. The experimentally measured coefficient of friction is transformed into $\bar{\mu}$ using the value of τ_0 obtained by fitting a thermal Maxwell-Eyring model to the measured data. $\bar{\tau}_c$ is obtained using the slip value given in the traction curve, the viscosity at the maximum Hertzian pressure as given by the Roelands equation, and the central film thickness given by Eq. (10).

The experimental results expressed in terms of $(\bar{\tau}_c, \bar{\mu})$ are displayed in Fig. 8. Regardless of variations in contact configurations or lubricant properties, the test results all fall rather closely on the mastercurve derived from the present numerical results. At this point it is noted that a reasonable agreement between theoretical and experimental results could be anticipated, because the latter results were taken from cases which were fitted to the Eyring model. However, it is still remarkable that experimental results obtained for widely different conditions can be brought together

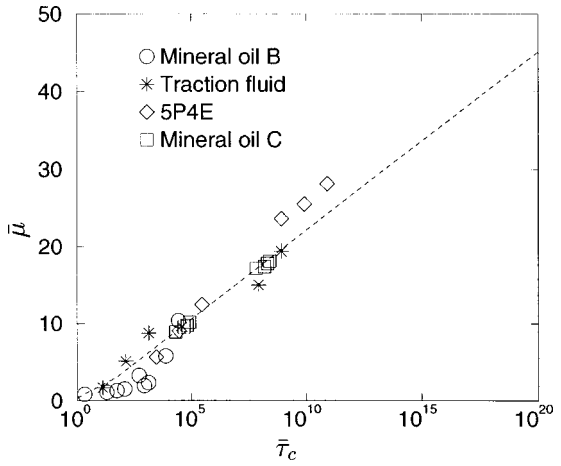

Fig. 8 Friction results obtained experimentally by Evans and Johnson [8,17] and Klein-Meuleman Lubrecht, and ten Napel [25] plotted using the friction parameters $\bar{\tau}_c$ and $\bar{\mu}$. Dashed curve: Eq. (13).

on a single curve by using $\bar{\tau}_c$. This makes a strong case for the combination $(\bar{\tau}_c, \bar{\mu})$ as parameters characterizing friction for the general case.

V Conclusions

The friction in smooth isothermal elliptic EHL contacts has been studied as a function of the operating conditions for the case of non-Newtonian lubricant behavior according to the Eyring model. It was found that the computed sliding friction values, when presented in the form of a generalized coefficient of friction as a function of a characteristic nondimensional shear stress, closely fall on a single curve that is accurately approximated by the following formula:

$$\bar{\mu} = \sinh^{-1}(\bar{\tau}_c/5). \tag{14}$$

This observed behavior seems to suggest the existence of a unifying mechanism determining the sliding friction in EHL contacts. By this it is meant that also when other rheological models are used e.g., a limiting shear stress model, one may expect to find a single curve $\bar{\mu} = \bar{\mu}(\bar{\tau}_c)$ but in that case the form of the curve will be different from Eq. (14). The validation of this assertion forms the topic of future research.

A formula such as Eq. (14) obviously forms a simple tool for engineering use to predict sliding friction as a function of operating conditions. However, because Eq. (14) is based on results assuming isothermal conditions, it should still be used with care. For cases where a significant amount of sliding occurs, the predicted coefficients of friction will be too large. The extension of the mastercurve to account for such shear heating effects forms another topic of future research.

Acknowledgments

The authors would like to thank Dr. H. Wittmeyer, Vice President SKF Group Technology Development, for his kind permission to publish this paper.

Appendix: Numerical Details

The equations presented in Sec. II A were discretized on a uniform grid with second order accuracy. A second order upstream discretization was used for the wedge term of the Reynolds equation, [Eq. (1)]. The discrete equations were then solved using multilevel techniques. These techniques were extensively described by Lubrecht [26] and Venner [24]. The second-order discretization of the wedge term was addressed by Venner and Lubrecht [27].

Table 4 Variation of the reduced friction coefficient with the discretization density

Level	H_c	$\bar{\mu}$
5 (64x64)	$3.545\ 10^{-3}$	42.38
6 (128x128)	$1.603\ 10^{-2}$	41.35
7 (256x256)	$1.978\ 10^{-2}$	41.13
8 (512x512)	$2.076\ 10^{-2}$	41.09

The numerical accuracy of the results is analyzed here for a specific case, a circular contact lubricated with the mineral oil A. The contact operates under a maximum Hertzian pressure of 3 GPa, an oil temperature of 40°C, and an average velocity of 12 m/s ($M = 1738$ and $L = 14.79$). The slip is taken to be 0.5 percent and the Eyring stress 4 MPa. Table IV presents the calculated reduced friction coefficient due to sliding friction together with the central film thickness as a function of the discretization density. The discretization density can also be expressed in terms of levels where level 1 has 4×4 points, level 2 has 8×8 points, etc. The friction coefficient appears to converge much faster than the central film thickness and the difference in friction between levels 6 and 5 is already barely 2.5 percent. Both, however, display a second-order convergence. While mainly concerned with the friction results and therefore satisfied with relatively low levels, level 7 was chosen in this work to provide, nevertheless, an accurate prediction of the film thickness. At this level, one may expect an error of about 5 percent for the film thickness and only 1 percent for friction.

Nomenclature

a = Hertzian contact length, $a = (3fR/E')^{1/3}(2\kappa\mathcal{E}/\pi)^{1/3}$.
b = Hertzian contact width, $b = a/\kappa$.
c = Hertzian approach, $c = (a^2/(2R))(\mathcal{K}/\mathcal{E})$.
D = Ellipticity ratio, $D = R_x/R_y$.
E': = Reduced modulus of elasticity, $2/E' = (1-\nu_1^2)/E_1 + (1-\nu_2^2)/E_2$.
$\mathcal{E}$ = Elliptic integral (second kind), $\mathcal{E} = \int_0^{\pi/2}(1-(1-\kappa^2)^2 \sin^2(\psi))^{1/2} d\psi$.
f = Nominal load.
H = Dimensionless film thickness, $H = h/c$.
H_c: = Dimensionless central film thickness (Moes), $H_c = h_c/R_x(\eta_0 u_s/(E'R_x))^{-1/2}$.
h = Film thickness.
$\mathcal{K}$ = Elliptic integral (first kind), $\mathcal{K} = \int_0^{\pi/2}(1-(1-\kappa^2)^2 \sin^2(\psi))^{-1/2} d\psi$.
L = Dimensionless lubricant parameter, $L = \alpha E'(\eta_0 u_s/(E'R_x))^{1/4}$.
M = Dimensionless load parameter, $M = f/(E'R_x^2)(E'R_x/(\eta_0 u_s))^{3/4}$.
$\mathcal{N}$ = Dimensionless parameter, $\mathcal{N} = \lambda p_H^2 \mathcal{K}/(6E'\tau_0)$.
P = Dimensionless pressure, $P = p/p_H$.
p = Pressure.
p_H: = Maximum Hertzian pressure, $p_H = 3f/(2\pi ab)$.
R = Reduced radius of curvature, $R^{-1} = R_x^{-1} + R_y^{-1}$.
R_x: = Reduced radius of curvature in the x direction, $R_x^{-1} = R_{x1}^{-1} + R_{x2}^{-1}$.
R_y: = Reduced radius of curvature in the y direction, $R_y^{-1} = R_{y1}^{-1} + R_{y2}^{-1}$.
S = Slide to roll ratio, $S = 2(u_2-u_1)/(u_2+u_1)$.
$\bar{S}$: = Dimensionless slip parameter, $\bar{S} = S(u_s \eta_0 E'/(\tau_0^2 R_x))^{1/2}$.
$\mathcal{S}$ = Shape factor, $\mathcal{S}(\kappa) = (\mathcal{E} - \kappa^2\mathcal{K})/(\mathcal{K} - \kappa^2\mathcal{K})$.

u_m = Average velocity, $u_m=(u_1+u_2)/2$.
u_s = Sum velocity, $u_s=u_1+u_2$.
u_1, u_2 = Velocity of the upper and lower surfaces.
X = Dimensionless coordinate, $X=x/a$.
Y = Dimensionless coordinate, $Y=y/b$.
x, y = Coordinates.
α = Pressure-viscosity coefficient.
$\overline{\alpha}$ = Dimensionless viscosity parameter, $\overline{\alpha}=\alpha p_H$.
Δ = Dimensionless mutual approach, $\Delta=\delta/c$.
δ = Mutual approach.
η = Viscosity.
η_0 = Viscosity at ambient pressure.
$\overline{\eta}$ = Dimensionless viscosity, $\overline{\eta}=\eta/\eta_0$.
$\overline{\eta}_X, \overline{\eta}_Y$ = Dimensionless effective viscosities, $\overline{\eta}_X=\eta_X/\eta_0$, $\overline{\eta}_Y=\eta_Y/\eta_0$.
κ = Ellipticity ratio, $\kappa=a/b$.
λ = Dimensionless speed parameter, $\lambda=(6\eta_0 u_s a)/(c^2 p_H)$.
μ = Friction coefficient.
$\overline{\mu}$ = Reduced friction coefficient, $\overline{\mu}=\mu p_H/\tau_0$.
ν_i = Poisson ratio of solid i.
τ_x, τ_y = Shear stresses in the x and y directions.
τ_e = Equivalent shear stress, $\tau_e=\sqrt{\tau_x^2+\tau_y^2}$.
τ_0 = Eyring stress.
τ_m = Mean shear stress.
$\overline{\tau}_c$ = Characteristic dimensionless shear stress, $\overline{\tau}_c=\overline{\eta}(p_H)\overline{S}/H_c$.
$\overline{\tau}_m$ = Dimensionless mean shear stress, $\overline{\tau}_m=\tau_m/\tau_0$.
$\overline{\tau}_x$ = Dimensionless shear stress in the x direction, $\overline{\tau}_x=\tau_x/\tau_0$.
ρ = Density.
ρ_0 = Density at ambient pressure.
$\overline{\rho}$ = Dimensionless density, $\overline{\rho}=\rho/\rho_0$.

References

[1] Dowson, D., and Higginson, G. R., 1966, *Elastohydrodynamic Lubrication, The Fundamentals of Roller and Gear Lubrication*, Pergamon Oxford.
[2] Hamrock, B., and Dowson, D., 1977, ''Isothermal Elastohydrodynamic Lubrication of Point Contacts, Part III-Fully Flooded Results,'' ASME J. Tribol., **99**, pp. 264–276.
[3] Lubrecht, A. A., and Venner, C. H., 1999, ''Elastohydrodynamic Lubrication of Rough Surfaces,'' Proc. Inst. Mech. Eng., Part J, **213**, pp. 397–404.
[4] Spikes, H. A., 1999, ''Thin Films in Elastohydrodynamic Lubrication: The Contribution of Experiment,'' Proc. Inst. Mech. Eng., Part J, **213**, pp. 335–352.
[5] Kaneta, M., and Kishikawa, H., 1999, ''Experimental Study on Microelastohydrodynamic Lubrication,'' Proc. Inst. Mech. Eng., Part J, **213**, pp. 371–382.
[6] Johnson, K. L., and Tevaarwerk, J. L., 1977, ''Shear Behavior of Elastohydrodynamic Oil Films,'' Proc. R. Soc. London, Ser. A, **356**, pp. 215–236.
[7] Bair, S., and Winer, W. O., 1979, ''A Rheological Model for Elastohydrodynamic Contacts Based in Primary Laboratory Data,'' ASME J. Tribol., **101**, pp. 258–265.
[8] Evans, C. R., and Johnson, K. L., 1986, ''Rheological Properties of EHD Lubricants,'' Proc. Inst. Mech. Eng., Part C: J. Mech. Eng. Sci., **200**, pp. 303–312.
[9] Jacobson, B., and Hamrock, B. J., 1984, ''Non-Newtonian Fluid Model Incorporated into Elastohydrodynamic Lubrication of Rectangular Contacts,'' ASME J. Tribol., **106**, pp. 275–284.
[10] Houpert, and L. G., Hamrock, B., 1986, ''Elastohydrodynamic Calculations as a Tool to Study Scuffing,'' *Proceedings of the 12th Leeds-Lyon Symposium on Tribology*, Tribology Series, Elsevier Amsterdam, pp. 146–155.
[11] Conry, T. F., Wang, S., and Cusano, C., 1987, ''A Reynolds-Eyring Equation for Elastohydrodynamic Lubrication in Line Contacts,'' ASME J. Tribol., **109**, pp. 648–658.
[12] Lee, R-T., and Hamrock, B. J., 1990, ''A Circular Non-Newtonian Model: Part I—Used in Elastohydrodynamic Lubrication,'' ASME J. Tribol., **112**, pp. 386–496.
[13] Sui, P. C., and Sadeghi, F., 1991, ''Non-Newtonian Thermal Elastohydrodynamic Lubrication,'' ASME J. Tribol., **113**, pp. 390–397.
[14] Hsiao, H.-S., and Hamrock, B. J., 1994, ''Non-Newtonian and Thermal Effects on Film Generation and Traction Reduction in EHL Line Contact Conjunctions,'' ASME J. Tribol., **116**, pp. 559–568.
[15] Kim, K. H., and Sadeghi, F., 1991, ''Non-Newtonian Elastohydrodynamic Lubrication of Point Contacts,'' ASME J. Tribol., **113**, pp. 703–711.
[16] Holt, C. A., Evans, H. P., and Snidle, R. W., 1996, ''Solution of the Non-Newtonian Elastohydrodynamic Problem for Circular Contacts Based on a Flow Continuity Method,'' Proc. Inst. Mech. Eng., Part J, **210**, pp. 247–258.
[17] Evans, C. R., and Johnson, K. L., 1986, ''Regimes of Traction in Elastohydrodynamic Lubrication,'' Proc. Inst. Mech. Eng., Part C: J. Mech. Eng. Sci., **200**, pp. 313–324.
[18] Olver, A., and Spikes, H. A., 1998, ''Prediction of Traction in Elastohydrodynamic Lubrication,'' Proc. Inst. Mech. Eng., Part J, **212**, pp. 321–332.
[19] Iivonen, H. T., and Hamrock, B. J., 1991, ''A Non-Newtonian Fluid Model Incorporated into Elastohydrodynamic Lubrication of Rectangular Contacts,'' Wear, **143**, pp. 297–305.
[20] Ehret, P., Dowson, D., and Taylor, C. M., 1998, ''On Lubricant Transport Conditions in Elastohydrodynamic Conjunctions,'' Proc. R. Soc. London, Ser. A, **454**, pp. 763–787.
[21] Greenwood, J. A., 2000, ''Two-dimensional Flow of a Non-Newtonian Lubricant,'' Proc. Inst. Mech. Eng., Part J, **214**, pp. 29–41.
[22] Roelands, C., 1966, *Correlational Aspects of the Temperature-Pressure Relationship of Lubrication Oils*, Ph.D. thesis, Technische Hogeschool Delft, The Netherlands.
[23] Moes, H., 1992, ''Optimum Similarity Analysis with Applications to Elastohydrodynamic Lubrication,'' Wear, **159**, pp. 57–66.
[24] Venner, C. H., 1991, *Multilevel Solution of the EHL Line and Point Contact Problems*, Ph.D. thesis, University of Twente, Enschede, The Netherlands.
[25] Klein Meuleman, P., Lubrecht, A. A., and ten Napel, W. E., 1985, ''Traction in Elastohydrodynamic Lubrication,'' University of Twente, Research Report No. WB 85–15.
[26] Lubrecht, A. A., 1987, *The Numerical Solution of Elastohydrodynamically Lubricated Line- and Point Contact Problem using Multigrid Techniques*, Ph.D. thesis, University of Twente, Enschede, The Netherlands.
[27] Venner, C. H., and Lubrecht, A. A., 1999, ''Amplitude Reduction of Non-Isotropic Harmonic Patterns in Circular EHL Contacts, under Pure Rolling,'' *Proceedings of the 25th Leeds-Lyon Symposium on Tribology*, Tribology Series 36, Elsevier, Amstardam, pp. 151–162.